 CMES, vol.89, no.3, pp.163-188, 2012

Predicting Leakage-induced Settlement of Shield tunnels in Saturated Clay

D.M. Zhang[1,2], L.X. Ma[1,2], H.W. Huang[1,2] and J. Zhang[1,2]

Abstract: This paper suggests a new set of analytical solutions for predicting leakage-induced seepage field and ground settlement in saturated clay. A unique feature of the solutions presented is considering the effect of the tunnel lining through the relative permeability between the tunnel and the soil. Through the superposition method, the proposed method can be easily extended to twin parallel tunnels. The accuracy of the analytical solutions are verified with numerical simulations. Parametric studies reveal that the decrease of pore pressure and the consequent settlements of ground and tunnel is proportional to the relative permeability. Over 20% of the initial hydrostatic pore pressure will dissipate when the relative permeability exceeds 0.01. The pore pressure decreases more significantly within the zone of 1.3D above the tunnel crown, 2.5D underneath the tunnel invert and 2.0D from the tunnel springline horizontally when the relative permeability is less than 0.01. Consequently, 62% of the total settlement of the ground occurs within this zone, which is called the main compression zone. It also shows that the tunnel leakage will result in very significant tunnel settlement because 78% of the total settlement occurs in the ground underlying the shield tunnel. Thus, the mechanism of the leakage-induced settlements of the ground and the tunnel can then be explained. For a typical shield tunnel in Shanghai, the leakage-induced settlement accounts for 1/6 of the total post-construction settlement.

Keywords: Analytical solution, Leakage, Shield tunnel, Saturated clay, Settlement

1 Introduction

Leakage is one of the key factors causing the settlement and deformation of tunnel built in the low-permeability saturated clay. In shield tunnels, leakage is often

[1] Department of Geotechnical Engineering, Tongji Univeristy, 1239 Siping Road, Shanghai 200092, China

[2] Key Laboratory of Geotechnical and Underground Engineeding of Minister of Education, 1239 Siping Road, Shanghai 200092, China

found at locations such as segmental joints, cracks and grouting holes, as shown in Fig. 1. When the water flows into the tunnel, pore water pressure will decrease and effective stress will increase, causing settlement of the tunnel and ground. How to predict the ultimate pore-water pressure induced by leakage is the key to assess the leakage-induced settlement. Many researches have studied the development of pore pressure due to tunnel leakage using numerical simulations [O'Reilly, Mair, and Alderman (1991); Shin, Addenbrooke, and Potts (2002); Shin (2010); Wongsaroj, Soga, and Mair (2007); Mair (2008); Xu, Shen, Chai, and Hong (2011)]. Moreover, some advanced numerical methods to study the seepage problem have also been developed [Peng, Cao, Dong, and Li (2011); Tatomir, Szymkiewicz, Class and Helmig (2011)]. As an important supplement to numerical simulation, analytical solutions have also been derived as they are simple to use and have clear physical meaning. Lei (1999) derived the solution for the pore water pressure distribution assuming that the hydraulic head at the ground surface and the tunnel perimeter are both constant. The approach is both suitable for shallow and deep tunnels. Based on Mobius-transformation and Fouries-series, El Tani (2003) provided a more general solution for tunnel with the hydraulic boundary condition of constant pore pressure. Kolymbas and Wagner (2006) presented a rigorous solution for a circular tunnel capable for both deep and shallow tunnels. Park, Owatsiriwong, and Lee (2007) derived the solutions for two different boundary conditions of constant water head and constant pore pressure. Huangfu, Wang, Tan, and Wang (2010) obtained the pore water pressure distribution by a different conformal mapping method assuming that the tunnel circumference is under a constant water head or constant water pressure. While these solutions provide useful insights into the leakage-induced pore pressure distribution under various boundary conditions, a common limitation in these studies is that the effect of permeability of tunnel lining is not considered for simplicity. For a shield tunnel built in saturated clay, the relative permeability between the tunnel and soil could significantly affect the seepage field and hence the resulting settlement due to the tunnel leakage [O'Reilly, Mair, and Alderman (1991); Shin, Addenbrooke, and Potts (2002); Wongsaroj (2005); Wongsaroj, Soga, and Mair (2007); Mair(2008)]. Thus, neglecting the effect of permeability of tunnel lining in the seepage analysis may not be appropriate. Another assumption commonly adopted in previous analytical solutions is the constant hydraulic head at the tunnel circumference as the boundary condition, which is actually an unknown parameter. However, little has been mentioned on how to determine this parameter.

This paper aimes to present a new set of analytical solutions for determining the ultimate leakage-induced pore pressure at the steady state, whereupon the leakage induced tunnel settlement is also studied. The new feature in the present analytical


Figure 1: Leakage of shield driven tunnel in Shanghai, China

solutions is that the effect of lining bas been considered. Furthermore, how to determine the constant hydraulic head boundary condition is discussed, which has been long ignored in the literature. The organization of this paper is as follows. First, the suggested analytical solutions for predicting the steady state pore water pressure considering tunnel leakage are introduced, based on which the procedure for tunnel settlement calculation is described. Then, the analytical solutions are verified with numerical simulations, followed by parametric studies to study how different factors could affect the leakage-induced pore pressure distribution as well as the settlement. Finally, the theory and method presented are applied to a real tunnel to study the impact of leakage-induced settlement to the total settlement.

2 Analytical solutions

2.1 Steady seepage state in the ground

Fig. 2 shows a tunnel in saturated clay. The external and internal diameter of the tunnel is R and r respectively. The depth from the water table to the tunnel center is h. The tunnel is embedded in saturated clay. The following assumptions are proposed to simplify the problem solution: (1) the tunnel is located in a fully saturated, homogeneous, isotropic, and semi-infinite clay; (2) the water is incompressible; (3) the water head on the external circumference of tunnel lining is h_a which is a variable in this paper.

According to Darcy's law and mass conservation, the two-dimensional flow around the tunnel can be described by Laplace equation as:

$$\frac{\partial^2 \varphi}{\partial x^2} + \frac{\partial^2 \varphi}{\partial y^2} = 0 \tag{1}$$

where φ is the total water head (or hydraulic head), which can be calculated based

on the position hydraulic head (Y) , the pore pressure (p) and the specific weight of water (γ_w) as:

$$\varphi = Y + \frac{p}{\gamma_w} \tag{2}$$

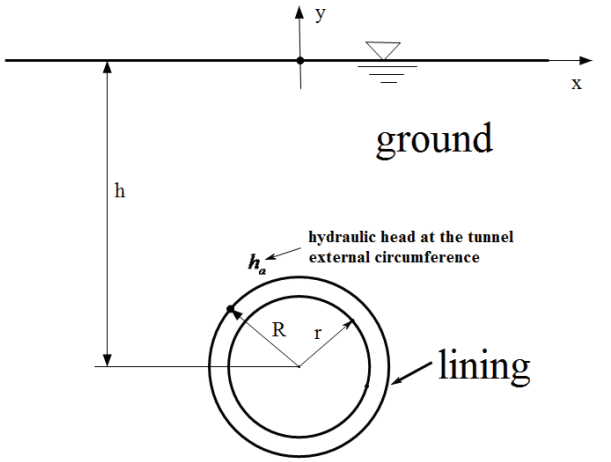

Figure 2: Circular tunnel in semi-infinite clay ground

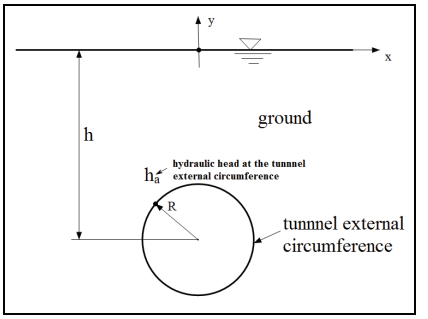

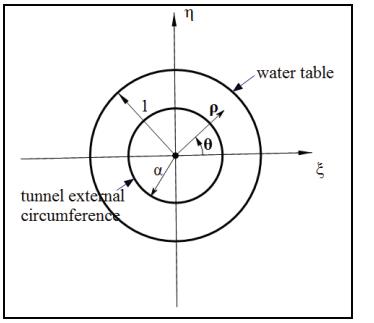

Figure 3: Method of conformal mapping

To solve the seepage field in soil mass, the conformal mapping technique (Fig.3) is used [Park, Owatsiriwong , and Lee (2008)]. In this study, the water table and the

external circumference of the lining in the $x-y$ plane can be mapped conformally onto two circles with a radius of unit one and α in the transformed $\xi-\eta$ plane. According to Verruijt and Booker (2000), the conformal transformation function for this problem can be described by Eq.3.

$$z = w(\varsigma) = -iA\frac{1+\varsigma}{1-\varsigma} \tag{3}$$

In the conformal mapping method, x and y in the rectangular coordinate system are related to ζ and η in the mapping coordinates through the following equations:

$$x = \frac{2A\eta}{(1-\xi)^2+\eta^2} \tag{4}$$

$$y = \frac{A(\xi^2+\eta^2-1)}{(1-\xi)^2+\eta^2} \tag{5}$$

where A and a are functions of geometric parameters of the tunnel as:

$$A = h(1-\alpha^2)/(1+\alpha^2) \tag{6}$$

$$\alpha = \frac{1}{R}(h-\sqrt{h^2-R^2}) \tag{7}$$

Based on the above relationships of conformal mapping, the governing function of Eq. (1) is still a Laplace function in $\xi-\eta$ plane, which can be rewritten as follows in the mapping coordinate system:

$$\frac{\partial^2\varphi}{\partial\xi^2}+\frac{\partial^2\varphi}{\partial\eta^2} = 0 \tag{8}$$

The analytical solution of Eq.6 can be written in terms of ρ and θ in a polar coordinate system in the $\zeta-\eta$ plane as:

$$\varphi = C_1 + C_2\ln\rho + \sum_{n=1}^{\infty}(C_3\rho^n + C_4\rho^{-n})\cos n\theta \tag{9}$$

where, C_1, C_2, C_3 and C_4 are constants to be determined by the drainage boundary condition at the water surface and the external circumference of the tunnel. Indeed, the water head at the external circumference of the tunnel is h_a and the water head at the water surface is 0, i.e., the boundary conditions can be written as follows in the $\zeta-\eta$ coordinate system:

$$\varphi(\rho = 1) = 0 \tag{10}$$

$$\varphi(\rho = \alpha) = h_a \tag{11}$$

Substituting Eqs.(8a) and 8(b) into Eq.(7), C_1, C_2, C_3 and C_4can be solved (See Appendix). Substituting the solved values of C_1, C_2, C_3 and C_4 into Eq. (7), the analytical solution for Eq.(7) with the boundary conditions of Eq.(8) can be obtained as:

$$\varphi = \frac{h_a}{\ln \alpha} \ln \rho \tag{12}$$

The rate of water flow into the tunnel from the soil mass can be obtained by integrating the seepage along the tunnel circumference as:

$$Q_s = k_s \int_0^{2\pi} \frac{\partial \varphi}{\partial \rho} \rho d\theta = \frac{2\pi k_s h_a}{\ln \alpha} = -\frac{2\pi k_s h_a}{\ln(\frac{h}{R} + \sqrt{\frac{h^2}{R^2} - 1})} \tag{13}$$

Where k_s= the permeability of the soil, h_a = the water head at the external circumference of the tunnel at the steady seepage state, h = the depth from the water table to the tunnel center, and R = the external diameter of the tunnel.

From Eq. 10, it can be found that Q_s is a function of the water head h_a, which is an unknown parameter to be determined but currently little knowledge is available on how to determine its value.

As will be shown later in this study, h_a could have significant effects on the predicted pore water pressure distribution and hence the leakage-induced settlement. Thus, a method is suggested to determine h_a based on the relationship of pore pressure and the water inflow rate for the axial symmetry of a circular tunnel instead of assuming a value for h_a subjectively, as adopted in many previous studies.

2.2 Determination of hydraulic head h_a and pore pressure at the steady stage

The water inflow rate into the tunnel from the soil mass (Eq.10) must be equal to the water inflow through the lining. Since the lining of the tunnel is axial-symmetric, a polar coordinate system with an original point at the tunnel center is used for convenience (Fig. 4). According to Darcy's law, the water inflow rate into the tunnel through the lining can be calculated as:

$$Q_l = k_l \int_0^{2\pi} \frac{\partial \varphi}{\partial \rho} \rho d\theta \tag{14}$$

Where, k_l is the permeability of the tunnel lining.

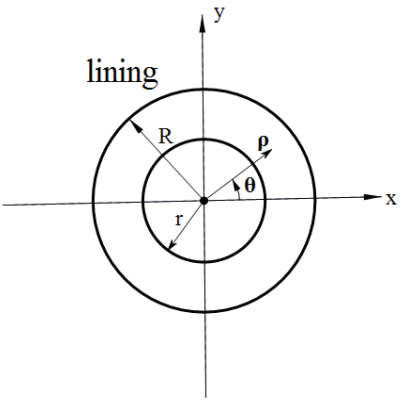

Figure 4: Polar coordinate system for the tunnel

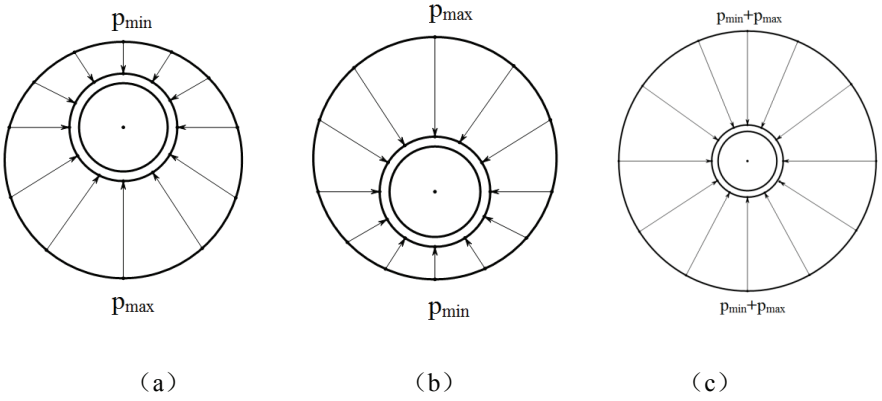

Figure 5: Superposition of the pore pressure

Substituting Eq.2 into Eq.11, Eq. 11 can also be expressed as:

$$Q_l = k_l \int_0^{2\pi} \frac{\partial(\rho \sin\theta + \frac{p}{\gamma_w})}{\partial \rho} \rho d\theta = k_l \int_0^{2\pi} \frac{1}{\gamma_w} \frac{\partial p}{\partial \rho} \rho d\theta \tag{15}$$

As Eq.12 indicates the water inflow rate into the tunnel only depends on the pore pressure p. Substituting Eq.2 into Eq. 1, Eq. 1 can also be expressed in terms of the pore water pressure$p$ as:

$$\frac{\partial^2 p}{\partial x^2} + \frac{\partial^2 p}{\partial y^2} = 0 \tag{16}$$

To solve Eq.13, the boundary conditions on the internal and external circumference of the tunnel should be determined. The pore pressure is 0 at the internal circumference, i.e., $p(\rho$=r) =0. At the external circumference of the tunnel, the water head is h_a in Fig. 2, and $h_a + h$ in the coordinate system of Fig. 4. Thus, the pore water pressure at the external circumference of the tunnel can be calculated as follows in the coordinate system of Fig. 4.

$$p(\rho = R) = (h_a + h - y) \times r_w \tag{17}$$

where h_a is the water head at the external circumference of the tunnel in the coordinate system of Fig.2, and h is the depth from the tunnel center to the water table.

However, it is quite difficult to solve Eq.13 analytically directly because the pore pressure at the external circumference as shown in Eq.14 is a function of y. A further examination of Eq. 14 shows that the pore pressure p at the external circumference boundary increases linearly with depth. Fig. 5(a) shows the pore water pressure distribution along the external circumference boundary as indicated by Eq. (14), where the pore pressure p_{min} and p_{max} are calculated using Eq.14. Fig. 5(b) shows a hypothetical boundary condition with pore pressure on the external surface of the tunnel symmetrical with that in Fig.5a about x-axis. As the tunnel is axial symmetrical, the pore pressure within the lining in Fig. 5b also satisfies Eq.12 and Eq.13 mathematically, which is symmetrical with the pore pressure within the lining in Fig. 5a about x-axis. As the water inflow rate into the tunnel only depends on the pore pressure p for the axi-symmetrical circular tunnel, the seepage from the two boundary conditions should be the same. Also, as p is a linear function of y, the superposition principle is applicable. We thus superpose the boundary conditions in Fig. 5(a) and Fig. 5(b) to produce a superposed condition as shown in Fig. 5(c), which can be written as follows:

$$p(\rho = R) = p_{\min} + p_{\max} = 2(h_a + h) r_w \tag{18}$$

$$p(\rho = r) = 0 \tag{19}$$

Considering the general solution form of Laplace's function shown as Eq.7, the solution for Eq.13 with the boundary condition Eq.15 is as:

$$p = -\frac{2(h_a+h)r_w \ln r}{\ln R - \ln r} + \frac{2(h_a+h)r_w}{\ln R - \ln r}\ln \rho \tag{20}$$

Substituting Eq.16 into Eq.12 and considering the superposition principle, the water inflow rate into the tunnel can be obtained by Eq.17.

$$Q_l = \frac{1}{2}k_l \int_0^{2\pi} \frac{\partial \varphi}{\partial \rho}\rho d\theta = \frac{2\pi k_l (h_a+h)}{\ln R - \ln r} \tag{21}$$

Since the water inflow into the tunnel from the soil mass should be the same as that flows through the lining, the water head $h_a$can be derived as follows by equating Eq.17 to Eq.10.

$$h_a = -\frac{hab}{(1+ab)} \tag{22}$$

in which, $a = k_l/k_s$ is the relative permeability between the lining and the soil mass. $b = \ln[h/R + (h^2/R^2 - 1)^{1/2}]/\ln(R/h)$ is a parameter concerning the geometries of the tunnel lining. Eq. 18 indicates that the ultimate pore pressure at the external circumference is closely related to the depth of the tunnel, the geometry of the tunnel, as well as the relative magnitude of permeability between the tunnel and the soil.

As has been shown previously, the water head, pore pressure and water flow rate are all functions of h_a. Since the value of h_a is known now, the water head, pore pressure distribution and water flow rate into the tunnel can be obtained as follows:

$$\varphi = -\frac{hab}{(1+ab)\ln \alpha}\ln \rho \tag{23}$$

$p = (-\frac{hab}{(1+ab)\ln \alpha}\ln \rho - y)\gamma_w$ or

$$p = [-\frac{hab}{(1+ab)\ln \alpha}\ln \sqrt{(\frac{x^2+y^2-A^2}{x^2+(y-A)^2})^2 + (\frac{2Ax}{x^2+(y-A)^2})^2} - y]\gamma_w \tag{24}$$

$$Q = \frac{2\pi k_s abh}{(1+ab)\ln(\frac{h}{R} + \sqrt{\frac{h^2}{R^2}-1})} \tag{25}$$

2.3 Prediction of leakage-induced settlement

The reduction of the pore pressure will increase the effective stress of soils and hence settlements of ground and the tunnel will result as well. The settlement at the ground surface d can be calculated by integrating the pore pressure dissipation induced as

$$d = \int_{-\infty}^{0} \varepsilon_y dy \tag{26}$$

Where ε_y is the vertical strain of the ground due to the pore pressure dissipation.

Supposing that the ground is still in the elastic state during the equilibrium of the pore pressure, the strain of the soil along the x, y, and z directions can be calculated as follows:

$$\varepsilon_x = \frac{1}{E}[\sigma_x - \mu(\sigma_y + \sigma_z)] \tag{27}$$

$$\varepsilon_y = \frac{1}{E}[\sigma_y - \mu(\sigma_z + \sigma_x)] \tag{28}$$

$$\varepsilon_z = \frac{1}{E}[\sigma_z - \mu(\sigma_x + \sigma_y)] \tag{29}$$

in which, E is Young's modulus, μ is Poisson's ratio, σ_x is the vertical gravity stress of the ground, σ_y and σ_z are the lateral stress of the ground.

The leakage does not induce settlement along the longitudinal direction of the tunnel, i.e.,

$$\varepsilon_z = 0 \tag{30}$$

Thus, the volume strain can be expressed as Eq.25.

$$\varepsilon_v = \varepsilon_x + \varepsilon_y \tag{31}$$

Substituting Eq.24 into Eq.23c, σ_z yields:

$$\sigma_z = \mu(\sigma_x + \sigma_y) \tag{32}$$

Substituting Eq.26 into Eq.23a and Eq.23b, Hooke's law can be rewritten as follows:

$$\varepsilon_x = \frac{1+\mu}{E}[(1-\mu)\sigma_x - \mu\sigma_y] \tag{33}$$

$$\varepsilon_y = \frac{1+\mu}{E}[-\mu\sigma_x + (1-\mu)\sigma_y] \tag{34}$$

For soft clay, the vertical stress is the soil gravity stress and the lateral stress are subordinated to vertial stress σ_x and can be calculated by Eq.28.

$$\sigma_x = K_0 \sigma_y \tag{35}$$

where, K_0 is the lateral pressure coefficient at rest, which can be written as:

$$K_0 = 1 - \sin\varphi \tag{36}$$

Where, φ is the effective internal friction angle of the soil.

Substituting Eq.28 into Eq.27 yields:

$$\frac{\varepsilon_x}{\varepsilon_y} = \frac{(1-\mu)K_0 - \mu}{-\mu K_0 + (1-\mu)} \tag{37}$$

Based on Eqs. 25 and Eq. 30, the vertical strain can be written as follows:

$$\varepsilon_y = \frac{-\mu K_0 + (1-\mu)}{(1-2\mu)(K_0+1)}\varepsilon_v \tag{38}$$

Since the mean stress of the ground is changed only due to the pore pressure dissipation, The volumetric strain can be calculated as:

$$\varepsilon_v = \frac{\Delta u}{K} = \frac{3(1-2\mu)\Delta p}{E} \tag{39}$$

in which, K is the bulk modulus, E is Young's modulus.

Substituting Eq.31 and Eq.32 into Eq.22, the leakage-induced ground settlement can then be expressed as:

$$d = \int_{-\infty}^{0} \frac{3(1-2\mu)(-\mu K_0 + (1-\mu))\Delta p}{(1-2\mu)(K_0+1)E} dy \tag{40}$$

According to Eq.20, the decrease of the pore pressure can be obtained from Eq.34.

$$\Delta p = \frac{hab\gamma_w}{(1+ab)\ln\alpha} \ln \sqrt{\left(\frac{x^2+y^2-A^2}{x^2+(y-A)^2}\right)^2 + \left(\frac{2Ax}{x^2+(y-A)^2}\right)^2} \tag{41}$$

The settlement of the tunnel is caused by soil compression below the tunnel. Consequently, the leakage-induced settlement of the tunnel is the same as the ground settlement underlying the tunnel. The integration in Eq.33 can be easily calculated using numerical integration software such as Matlab.

2.4 Extension of the analytical solution to twin parallel tunnels

In fact, most shield-driven tunnels are constructed in pair as shown in Fig.6. The proposed analytical solution is derived for a single tunnel, but it can be extended for analyzing twin tunnels using the superposition method, i.e., the seepage field caused by leakage in twin tunnels is the summation of the seepage field caused by a single tunnel. As will be seen, the seepage field obtained based on such a superposition method can indeed be quite accurate.

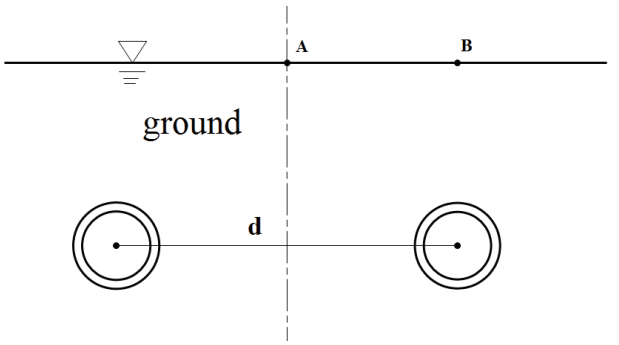

Figure 6: Twin parallel tunnels in the ground

3 Validation of the analytical solution

3.1 Validation for a single tunnel

A numerical simulation is adopted to validate the analytical solution for the pore water pressure distribution since it is the key for settlement prediction. In the numerical model, the shield tunnel is located at a depth of 15m from the tunnel center. The water table is at the ground surface. The outer and inner diameters are 6.2m and 5.5m respectively. The thickness of the tunnel lining is 350mm. The permeability of the soil and the tunnel lining are adopted as 10^{-9}ms^{-1} and 10^{-11}ms^{-1}, respectively, i.e., the relative permeability between the tunnel and the soil is 0.01. The pore pressure at the inner circumference of the tunnel is 0. The seepage is analysed using the finite element software ABAQUS, as shown in Fig.7. Both the soil and tunnel lining are simulated as solid elements.

Fig.8 and Fig.9 show the predicted pore water pressure predicted from the analytical solution and the numerical simulation, respectively. Generally, the two solutions for pore pressure match quite well for points apart from the numerical boundaries. The most significant deviation of the two solutions for pore pressure occurs at the

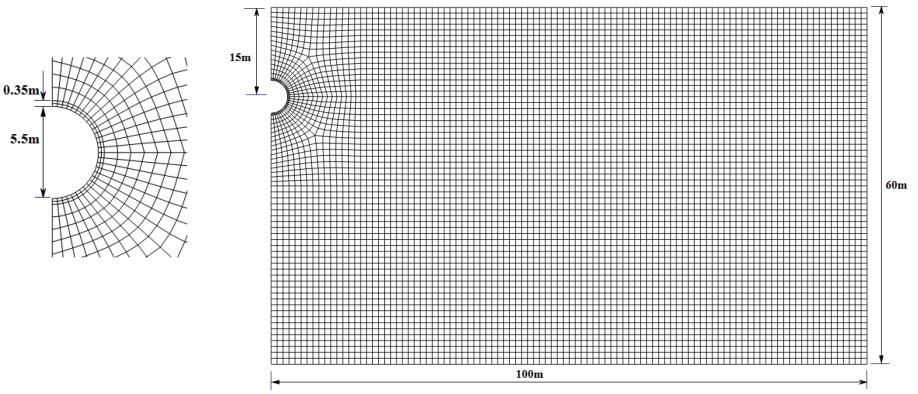

Figure 7: Numerical simulation model

tunnel crown where the predicted pore water pressure from the analytical solution is 4% lower than that from the numerical simulation. In this example, the relative permeability used is 0.01, which is almost the upper limit for a shield tunnel in saturated clay. This thus verifies the suggested analytical solutions for pore water pressure prediction. Further parametric studies on relative permeability indicate that the difference between the numerical and analytical solutions diminishes as the relative permeability decreases, i.e., the analytical solution could be more accurate as the relative permeability diminishes.

3.2 Validation for twin parallel tunnels

By the superposition method, the analytical solution of the seepage field for a single tunnel can also be extended to the case of twin parallel tunnels, which is common in practice. To validate this idea, a comparison between the analytical solution and the numerical solution has also been carried out. In the numerical model, the depth of the two parallel tunnels is 15 m from the tunnel center to the ground surface. The water table is at the ground surface. The permeability of the soil and the tunnel are 10^{-9}ms^{-1} and 10^{-11}ms^{-1} respectively. The two tunnels are 13 m (about 2.1D) apart from center to center. The numerical model is shown in Fig.10. For ease of comparison, some reference points are first selected, as shown in Fig.11.

Figs. 12(a) - (g) compare the pore water pressure predicted from numerical and analytical solutions. Generally, the two sets of solutions agree well for points apart from the tunnel boundaries. The largest deviation is observed at the crown of the tunnel (point 2) where the analytical solution is about 7% less than the numerical

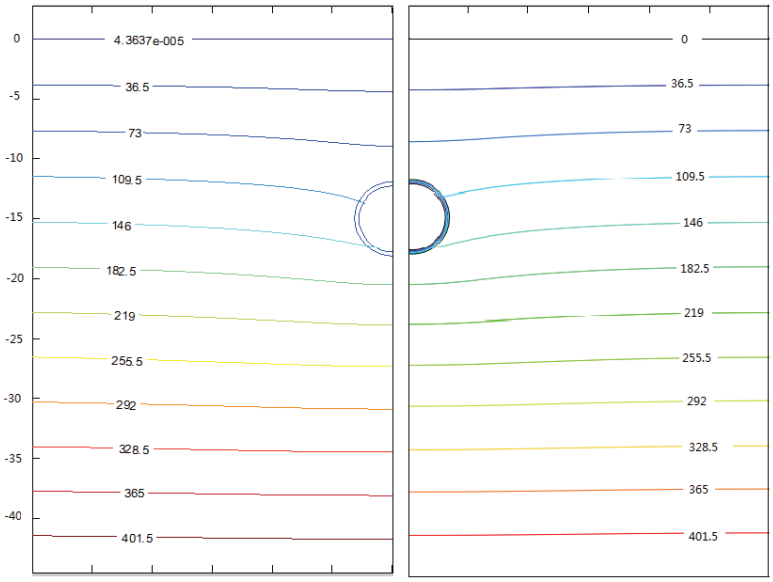

Figure 8: Comparison between the analytical solution (left) and numerical solution (right) for the pore pressure distribution in soil mass around the tunnel

results. Thus, the proposed method can also be used for analysing leakage induced pore water pressure distribution in the case of twin tunnels.

4 Parametric studies

4.1 Effect of relative permeability on pore pressure distribution

Previously, the effect of tunnel lining has been ignored in predicting the pore water pressure distribution. With the analytical solutions presented in this study, the effect of tunnel lining can be considered with the relative permeability. The relative permeability between the tunnel and the soil is proposed here in the large range of 0.001 to 0.01 to study the its effect on pore pressure distribution around the tunnel. To investigate the effect of relative permeability, the pore water pressure around a hypothetical tunnel is first calculated under three cases, as summarised in Table 1. In this Table, the water head h_a at the external circumference at the steady seepage state is determined using Eq.18, We can see that h_a is quite sensitive to the relative permeability: the water head h_a increases about 10 times when the relative permeability changes from 0.001 to 0.01.

Figs. 13-15 show the decrease of pore pressure in the ground at different locations

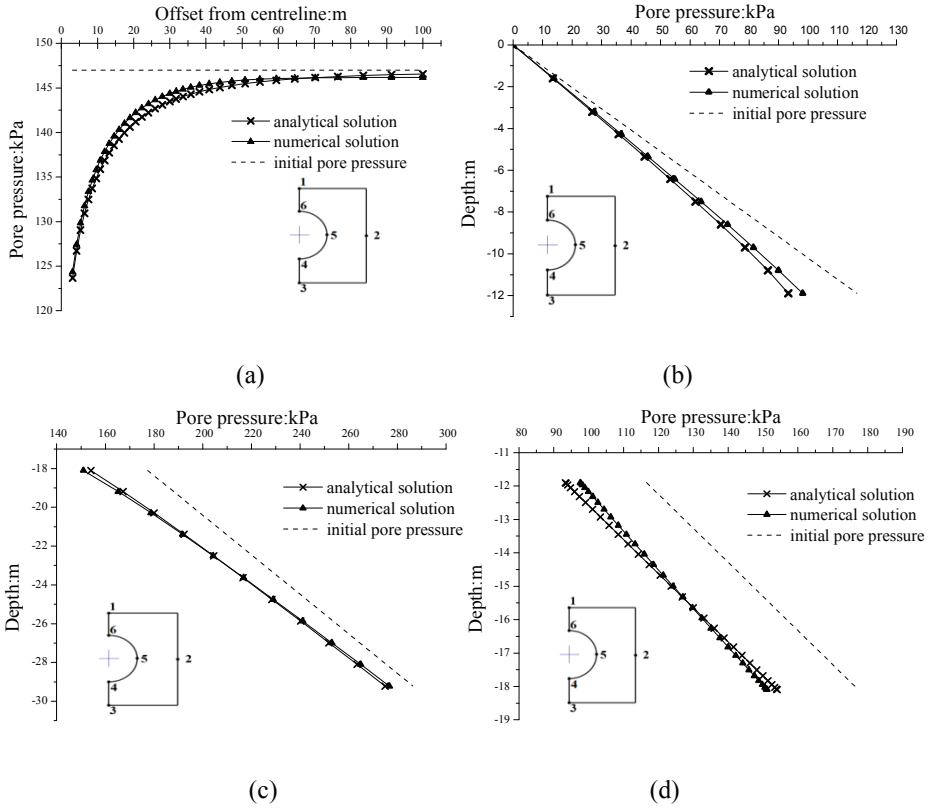

Figure 9: Comparison between solutions for pore pressure:(a) at the tunnel's spring line(5-2); (b) above the tunnel crown(1-6);(c) below the tunnel(4-5); (d) along the external circumference of the lining (6-5-4)

for the three cases as listed in Table 1. Fig. 13a shows that along the line above the tunnel crown the most significant decrease of the pore pressure occurs at the tunnel crown. When the relative permeability is 0.001, 0.005 and 0.01, the pore pressure decreases from 119 kPa to 116 kPa, to 106 kPa, and to 95 kPa, respectively. We can see that the decrease of the pore pressure at the tunnel crown is proportional to the relative permeability, and that over 20% of the initial hydrostatic pressure will dissipate when the relative permeability exceeds 0.01. This means that the relative permeability between the tunnel and the soil plays a very important role in the equilibrium process of pore pressure due to the tunnel leakage. Fig.13a also shows that above the tunnel crown the pore pressure decrease is much more significant within the zone of 1.3D (D is the outer diameter of the tunnel), indicating

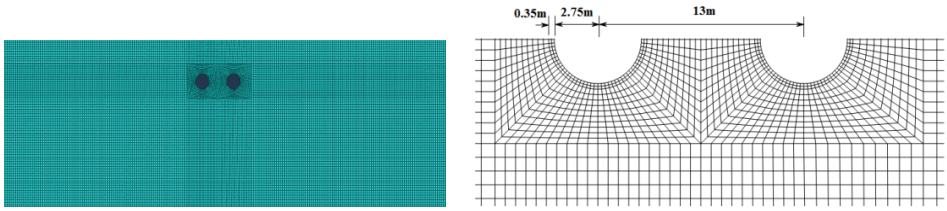

Figure 10: Numerical model for two parallel tunnels

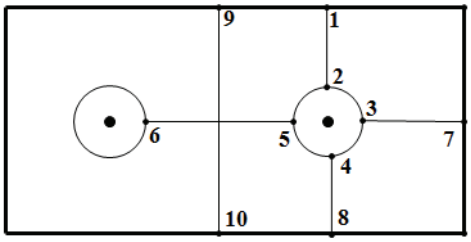

Figure 11: Reference points for comparison

an increase of effective stress and the settlement also mainly lies in this zone.

Table 1: Parameters used to study the pore pressure distribution

case	h(m)	R(m)	r(m)	k_l(ms^{-2})	k_s(ms^{-2})	h_a(m)
1	15	3.1	2.75	10^{-11}	10^{-9}	-2.3797
2	15	3.1	2.75	5×10^{-12}	10^{-9}	-1.2923
3	15	3.1	2.75	10^{-12}	10^{-9}	-0.2776

The decrease of pore pressure below the tunnel invert is illustrated in Fig. 13b. When the relative permeability is 0.001, 0.005 and 0.01, the maximum pore pressure decreases from 181 kPa to 178 kPa, to 168 kPa, and to 157 kPa, respectively. The amount of pore water pressure dissipation is about 13% when the relative permeability is 0.01. In this figure, the most significant pore pressure dissipation is within the area of 2.5D below the tunnel invert, which is almost two times as that above the tunnel crown [See Fig. 14(a)].

The drawdown of the pore pressure at the tunnel springline is shown in Fig.14a. When the relative permeability is 0.001, 0.005 and 0.01, the maximum pore pressure decreases from 150 kPa to 147 kPa, to 137 kPa, and to 126 kPa, respectively.

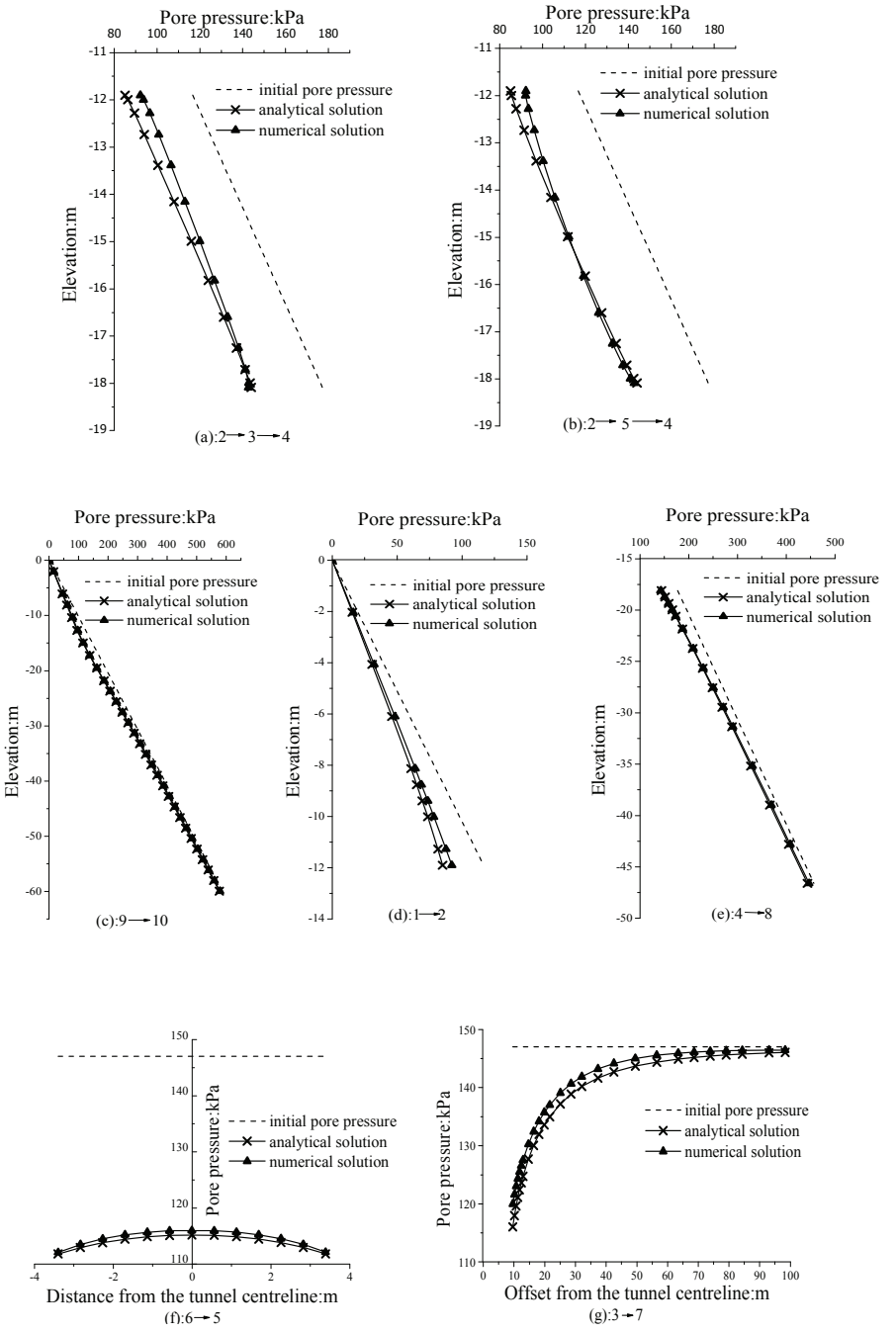

Figure 12: Comparison between analytical and numerical solutions

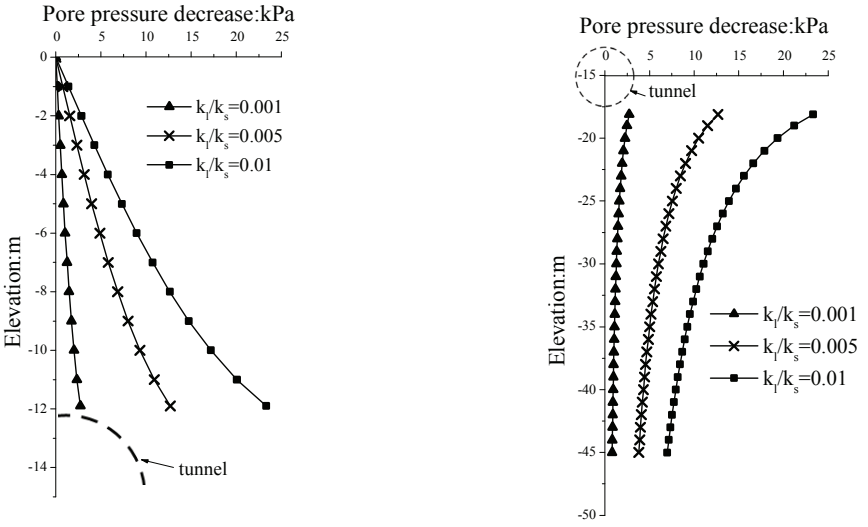

(a) above the tunnel crown (b) underneath the tunnel invert

Figure 13: Decrease of pore pressure with relative permeability above and underneath the tunnel

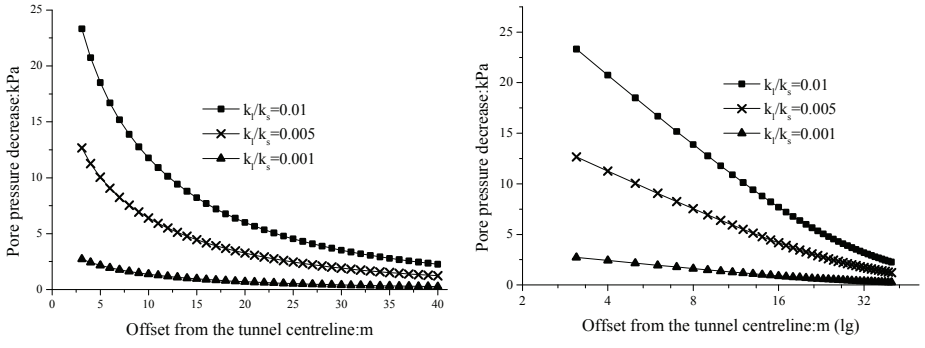

(a) (b)

Figure 14: Evolution of pore pressure with relative permeability at the tunnel springline level

The ultimate dissipation of the pore pressure reaches 16% of the initial pore pressure when the relative permeability is 0.01. The pore pressure drawdown mainly occurs within the zone of 2.0D from the tunnel springline. Comparing Figs 13(a), 13(b) and 14(a), we can see that the leakage induced pore pressure dissipation is confined in a relatively small region around the tunnel.

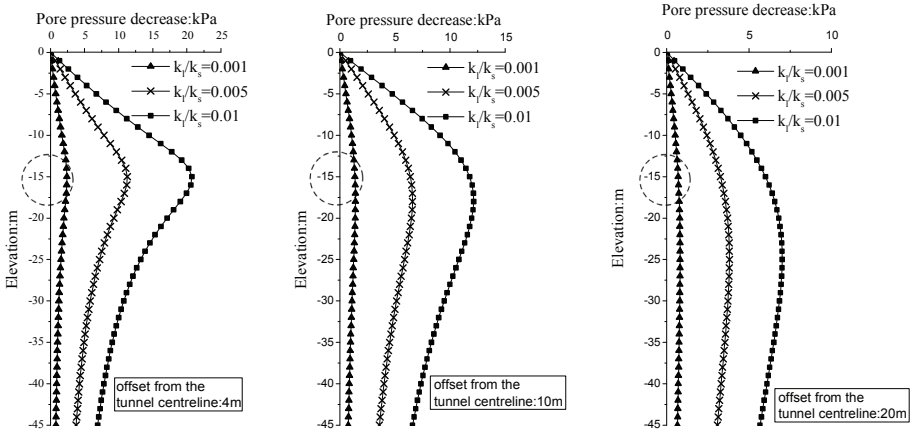

Figure 15: Pore pressure decrease at different vertical planes from the tunnel centre

Fig. 15 shows the decrease of the pore pressure at vertical planes with different distances from the tunnel as the relative permeability varies. When the relative permeability is 0.01 and when the vertical plane is 1m, 1D, and 2.7D from the tunnel centre, the maximum pore pressure change is 90%, 53%, and 31% of the maximum pore pressure change along the springline, indicating the pore pressure change gradually reduces as the distance from the tunnel increases. For comparison on the relative permeability is 0.001, the maximum pore pressure change is 81%, 47%, and 27% of the maximum pore pressure change along the spring line, respectively. It seems that a larger relative permeability will tend to produce more pore pressure dissipation in a larger affected zone, but the size of the affected zone is not very sensitive to the relative permeability. Moreover, for the three vertical planes studied in Fig.15, the maximum pore pressure decrease is at 0.5D and 1.6D below the centreline of the tunnel, indicating that the maximum decrease of the pore pressure moves deeper when the vertical plane moves away from the tunnel.

In summary, the leakage-induced drawdown of the pore pressure mainly occurs within the zone defined by 1.3D from the crown, 2.0D from the springline, and 2.5D from the invert of the tunnel. The size of the zone with significant pore pressure

change is not very sensitive to the relative permeability. The size of the zone with significant pore pressure change may have important implication on analysing the seepage field of twin tunnels. For instance, when the centre-to-centre distance of two parallel tunnels is more than 5.0D, the interaction between leakage-induced seepage fields of the two parallel tunnels might be neglible.

4.2 Influence of relative permeability on settlement

To study the effect of relative permeability on settlement, a typical shield tunnel in Shanghai has been analysed for three cases using parameters listed in Table 2. Fig. 16 shows the calculated settlements above the tunnel crown and below tunnel invert with various relative permeability. Fig. 17 shows the settlement profile along various vertical planes with different distances from the tunnel centre.

Table 2: Parameters used to calculate the settlement

case	h(m)	R(m)	r(m)	k_l(ms^{-2})	k_s(ms^{-2})	h_a(m)	E_s(MPa)	μ	K_0
1	15	3.1	2.75	10^{-11}	10^{-9}	-2.3797	5	0.4	0.7
2	15	3.1	2.75	5×10^{-12}	10^{-9}	-1.2923	5	0.4	0.7
3	15	3.1	2.75	10^{-12}	10^{-9}	-0.2776	5	0.4	0.7

Figs. 16 and 17 show that the relationship between settlement and relative permeability is similar to the relationship between pore pressure change and relative permeability, which is reasonable since an elastic constitutive model is assumed in the settlement calculation. When the relative permeability varies from 0.001, to 0.005 and to 0.01, the leakage-induced surface settlement above the tunnel crown is 6 mm, 27 mm and 50 mm, respectively, and the leakage–induced settlement of the tunnel is 4.5 mm, 21 mm and 38 mm, respectively. Comparing Fig.16a and Fig.16b, it can be detected that only 22% of the total ground settlement takes place above the tunnel crown, while 78% of the total settlement comes from the compression of the ground below the tunnel invert. This appearance provides a hint the tunnel leakage will result in an inevitable and probably a significant tunnel settlement even if this will depend on the relative permeability between the tunnel and the soil.

Generally, the ground can be classified into three parts on the basis of the settlement distribution along the depth. The first part is marked by the shadow as shown in Fig. 17a and called the main compression zone as 62% of the total ground settlement occurs within this region of 1.3D from the tunnel crown, 2.5D below the tunnel

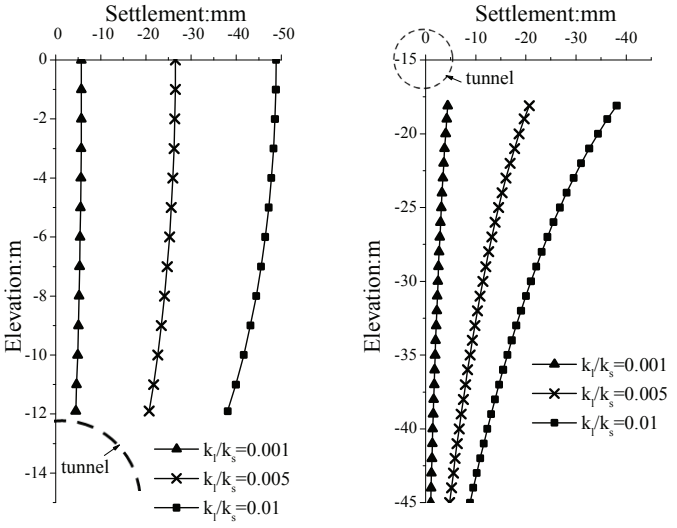

(a) (b)

Figure 16: Development of ground settlement with various relative permeability (a) above and (b) below the tunnel

invert and 2.0D from the tunnel springline. The second part is the area below the shadow area and marked as the secondary compression zone. The compression of the ground in the secondary compression zone accounts for 34% of the total settlement. The third part is the region above the shadow area called the rigid movement zone. Only 4% of the total settlement takes place within this zone. The soil in this region almost moves like a rigid body. The distribution of the settlement along the depth implies that the tunnel will be squatted down due to leakage because most of the settlement occurs within the main compression zone. Mair (2008) also observed the long-term squatting of shield tunnels.

5 Field application

Many different factors are likely to contribute to the long-term settlement of shield tunnels. The contribution from leakage-induced settlement to the total settlement has been of interest to many researchers and practicing engineers. The present analytical solution could help address this concern. To illustrate this point, a section of a typical shield-driven tunnel in Shanghai has been studied. The tunnel is located 11m under the ground from the tunnel centre with an outer radius of 3.1 m and an

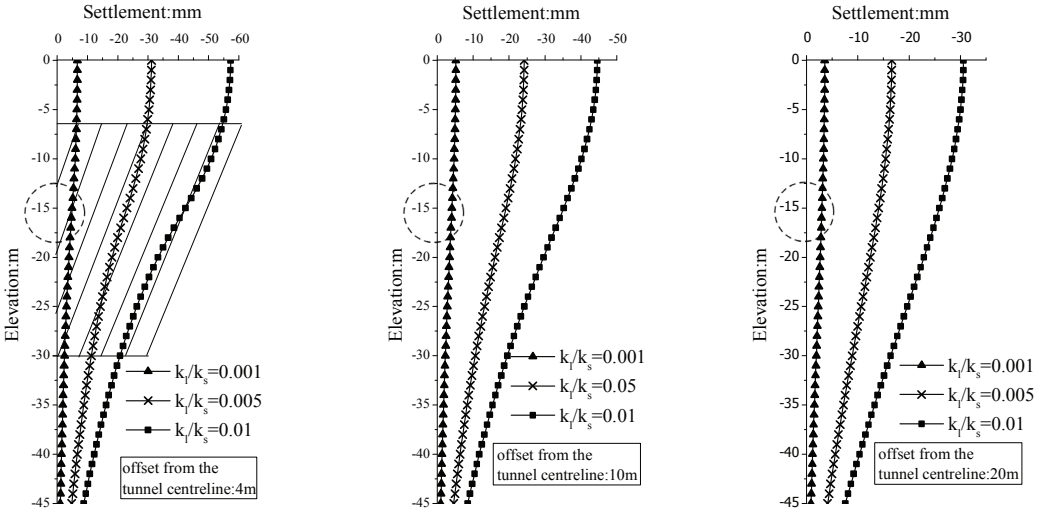

(a) (b) (c)

Figure 17: Ground settlement with various relative permeability at different profiles from the tunnel :(a) 4m offset from the tunnel centre, (b) 10m offset from the tunnel centre, (c) 20m offset from the tunnel centre

inner radius of 2.75 m. It is embedded in the saturated clay and the permeability of the clay is 5.4×10^{-9}ms^{-1}. The water table is about 0.5 m below the ground surface. The observed tunnel settlement of this section is shown in Fig.18. A special feature of this tunnel is that the measurement of settlement lasted for 10 years after the completion of the tunnel. The ultimate settlement is about 60 mm.

In Shanghai, the water inflow rate in shield tunnels is controlled to be less than 0.1 Lm^2/d. Assuming an inflow rate of 0.1 Lm^2/d , the permeability of the tunnel is about 2.25×10^{-11}ms^{-1} with Eq. 17. The relative permeability between the tunnel and the soil is thus 0.004. The Young's modulus, Poisson's ratio and the lateral earth pressure coefficient at rest of the soil is 5000 kPa, 0.4 and 0.7 respectively. The interaction between parallel tunnels has not been considered since their centre-to-centre distance is larger than 5.0 D where the effect of interaction is negligible. With the proposed analytical solution presented in this study, the leakage-induced settlement of the tunnel is 10 mm, which is about 1/6 of the total long-term settlement. In reality, the inflow rate is very difficult to control exactly. If the actual inflow rate is larger than 0.1 Lm^2/d, the leakage-induced settment would be larger

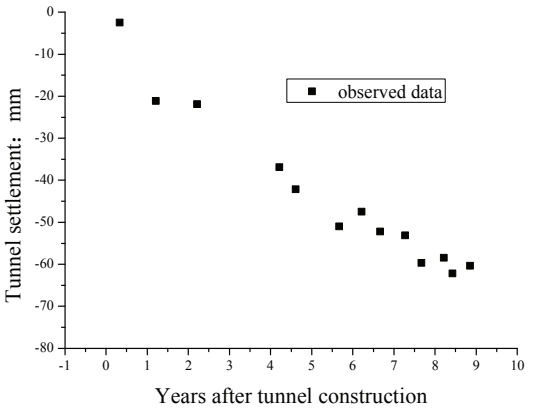

Figure 18: The observed long-term tunnel settlement of a section in Shanghai

than 10 mm, and vice versa.

6 Conclusions

This paper suggests an analytical solution for predicting the leakage-induced seepage field for shield tunnels in saturated clay , based on which the leakage-induced settlement of the ground and the tunnel can be assessed. For the tunnels studied in this paper, the following conclusions can be drawn:

(1) The relative permeability between the tunnel and the soil plays a very important role in the equilibrium process of pore pressure due to tunnel leakage. The decrease of the pore pressure around the tunnel and the resulting settlement of ground and tunnel are both proportional to the relative permeability.

(2) The pore pressure decreases significantly within the zone of 1.3D above the tunnel crown, 2.5D below the tunnel invert and 2.0D from the tunnel springline when the relative permeability is less than 0.01. Over 20% of the initial hydrostatic pore pressure could dissipate due to leakage when the relative permeability exceeds 0.01.

(3) Corresponding to the pore pressure dissipation characteristics, the ground can be classified into three parts, i.e., the main compression zone, the secondary compression zone, and the rigid movement zone. The main compression zone is within the range of 1.3D above the tunnel crown, 2.5D below the tunnel invert and 2.0D from the tunnel springline. 62% of the total ground settlement occurs within the main compression zone.

(4) Tunnel-leakage will result in significant tunnel settlement because 78% of the

total settlement occurs in the underlying ground of the tunnel and only 22% of the total ground settlement takes place above the tunnel crown. For a typical shield tunnel in Shanghai, the leakage-induced settlement accounts for 1/6 of the total post-construction settlement.

Acknowledgement: This study was substantially supported by the Natural Science Foundation of China (No.51278379), National Basic Research Program of China (973 Program: 2011CB013800), Natural Science Foundation of Shanghai (No.12ZR1433600), and the Program for Changjiang Scholars and Innovative Research Team in University (PCSIRT, IRT1029).

References

El Tani, M. (2002): Circular tunnel in a semi-infinite aquifer. *Tunnelling and Underground Space Technology*, vol. 18, no. 1, pp. 49-55.

Huangfu, M.; Wang, M. S.; Tan, Z.; Wang, X. Y. (2010): Analytical solutions for steady seepage into an underwater circular tunnel. *Tunnelling and Underground Space Technology*, vol. 25, no. 4, pp. 391-396.

Kolymbas, D.; Wagner, P. (2007): Groundwater ingress to tunnels - the exact analytical solution. *Tunnelling and Underground Space Technology*, vol. 22, no. 1, pp. 23-27.

Lei, S. (1999): An analytical solution for steady flow into a tunnel. *Ground Water*, vol. 37, no. 1, pp. 23-26.

Mair, R. J. (2008): Tunnelling and geotechnics: new horizons. *Geotechnique*, vol. 58, no. 9, pp. 695-736.

O'Reilly, M. P.; Mair, R. J.; Alderman, G. H. (1991): Long-term settlements over tunnels: an eleven-year study at Grimsby. *Proceedings of Conference Tunnelling, London, Institution of Mining and Metallurgy*, pp. 55-64.

Park, K. H.; Owatsiriwong, A.; Lee, J. G. (2008): Analytical solution for steady-state groundwater inflow into a drained circular tunnel in a semi-infinite aquifer: A revisit. *Tunnelling and Underground Space Technology*, vol. 23, no. 2, pp. 206-209.

Peng, W. H.; Cao, G. H.; Dong, Z. Z.; Li, S. C. (2011): Darcy-Stokes equations with finite difference and natural boundary element coupling method. *CMES: Computer Modeling in Engineering & Sciences*, vol. 75, no. 3, pp. 173-188.

Shin, J. H.; Addenbrooke, T. I.; Potts, D. M. (2002): A numerical study of the effect of groundwater movement on long-term tunnel behavior. *Geotechnique*, vol. 52, no. 6, pp. 1585-1599.

Shin, J. H. (2010): Analytical and combined numerical methods evaluation pore pressure on tunnels. *Geotechnique*, vol. 60, no. 2, pp. 141-145.

Tatomir, A.B.; Szymkiewicz, A.; Class, H.; Helmig, R. (2011): Modeling two phase flow in large scale fractured porous media with an extended multiple interacting continua method. *CMES: Computer Modeling in Engineering & Science,* vol. 77, no. 2, pp. 81-112.

Verruijt, A.; Booker, J. R. (2000): Complex variable analysis of Mindlin's tunnel problem. *Development of Theoretical Geomechanics, Sydney, 3-22, Balkema.*

Wongsaroj, J. (2005): Three-dimensional finite element analysis of short and long-term ground response to open-face tunnelling in stiff clay. *PhD thesis*, *University of Cambridge*.

Wongsaroj, J.; Soga, K.; Mair, R. J. (2007): Modelling of long-term ground response to tunnelling under St James' Park, London. *Geotechnique*, vol. 57, no. 1, pp. 75-90.

Xu, Y. S.; Shen, S. L.; Chai, J. C.; Hong, Z. S. (2011): Analysis of cutoff effect on groundwater seepage of underground structures in Aquifers of Shanghai. *ICCES: International Conference on Computational & Experimental Engineering & Sciences*, vol. 20, no. 2, pp. 65

Appendix

C_1, C_2, C_3, C_4 are the paramters that needed to be determined in Eq. (a1) as follows:

$$\varphi = C_1 + C_2 \ln \rho + \sum_{n=1}^{\infty} (C_3 \rho^n + C_4 \rho^{-n}) \cos n\theta \tag{a1}$$

The boundary conditions of Eq. (a1) is as follows:

$$\varphi(\rho = 1) = 0 \tag{a2}$$

$$\varphi(\rho = \alpha) = h_a \tag{a3}$$

Substituting Eq.(a2) into Eq.(a1) yields:

$$\varphi(\rho = 1) = C_1 + \sum_{n=1}^{\infty} (C_3 + C_4) \cos n\theta = 0 \tag{a4}$$

The variable θ in Eq. (a4) is within the range of 0-2π. To make sure that Eq.(a4) can be satisfied for any value of θ within the range of 0-2π, $C_1 C_3$ and C_4 is subordinated to the follows:

$$C_1 = 0 \tag{a5}$$

$$C_3 = -C_4 \tag{a6}$$

Substituging Eq. (a5) and Eq. (a6) in to Eq. (a1), φ can be written as:

$$\varphi = C_2 \ln \rho + \sum_{n=1}^{\infty} (C_3 \rho^n - C_3 \rho^{-n}) \cos n\theta \tag{a7}$$

Substituting Eq.(a3) into Eq.(a7) yields:

$$\varphi(\rho = \alpha) = C_2 \ln \alpha + \sum_{n=1}^{\infty} C_3 (\alpha^n - \alpha^{-n}) \cos n\theta = \varphi_0 \tag{a8}$$

To satisfy Eq. (a8) for any value of θ within the range of 0-2π, C_3 and C_4 must be subordinated to the follows:

$$C_3 = 0 \tag{a9}$$

$$C_2 = \frac{\varphi_0}{\ln \alpha} \tag{a10}$$

Thus, with the boundary conditions of Eq. (a2) and Eq. (a3), the paramters of C_1, C_2, C_3 and C_4 are determined as follows:

$$\begin{cases} C_1 = 0 \\ C_2 = \frac{\varphi_0}{\ln \alpha} \\ C_3 = 0 \\ C_4 = 0 \end{cases} \tag{a11}$$